

The novel p53 target TNFAIP8 variant 2 is increased in cancer and offsets p53-dependent tumor suppression

Julie M Lowe^{*1}, Thuy-Ai Nguyen², Sara A Grimm³, Kristin A Gabor¹, Shyamal D Peddada³, Leping Li³, Carl W Anderson², Michael A Resnick², Daniel Menendez^{2,4} and Michael B Fessler^{*1,4}

Tumor necrosis factor- α -induced protein 8 (*TNFAIP8*) is a stress-response gene that has been associated with cancer, but no studies have differentiated among or defined the regulation or function of any of its several recently described expression variants. We found that *TNFAIP8* variant 2 (v2) is overexpressed in multiple human cancers, whereas other variants are commonly downregulated in cancer (v1) or minimally expressed in cancer or normal tissue (v3–v6). Silencing v2 in cancer cells induces p53-independent inhibition of DNA synthesis, widespread binding of p53, and induction of target genes and p53-dependent cell cycle arrest and DNA damage sensitization. Cell cycle arrest induced by v2 silencing requires p53-dependent induction of p21. In response to the chemotherapeutic agent doxorubicin, p53 regulates v2 through binding to an intragenic enhancer, together indicating that p53 and v2 engage in complex reciprocal regulation. We propose that *TNFAIP8* v2 promotes human cancer by broadly repressing p53 function, in essence offsetting p53-dependent tumor suppression.

Cell Death and Differentiation (2017) 24, 181–191; doi:10.1038/cdd.2016.130; published online 11 November 2016

Tumor necrosis factor- α -induced protein 8 (*TNFAIP8*) is the founding member of a recently described family of environmental stress response genes that are induced by TNF α . *TNFAIP8* has been shown to promote or inhibit apoptosis, depending on cell type and context.^{1,2} Although little is known about *TNFAIP8*, it has recently been found to be overexpressed in a wide range of human cancers. Some studies have suggested protumor functions for *TNFAIP8*, including enhancement of cell survival, proliferation, and metastasis^{3–9} and resistance to cancer chemotherapeutics in mice.^{4,10} Nonetheless, nothing is known about how *TNFAIP8* influences responses to DNA damage in cancer cells. Moreover, several transcript variants from the *TNFAIP8* gene were recently registered in the NCBI reference sequence database, but no study to date has differentiated among them or defined the factors that govern their expression.

The tumor suppressor p53 is a transcription factor that regulates many biological processes through its target gene network. Some of the well-characterized p53 target genes including p21/*CDKN1A*, *growth arrest and DNA damage-inducible 45a* (*GADD45A*) and *Bcl-2-like protein 4* (*BAX*) together promote senescence, cell cycle arrest, and apoptosis, all of which may contribute to the tumor suppressing functions of p53.^{11,12} Additional noncanonical tumor-suppressive pathways from p53 have recently been

identified.^{13–15} Improved characterization of the p53 DNA-binding sequence with modern sequencing techniques has led to the identification of a rapidly expanding list of p53 target genes.^{16–18} Continued identification of these genes and characterization of their mechanisms of regulation and function will be critical to a full understanding of p53 and for full realization of opportunities to intervene upon p53 in cancer.

Here, we identify *TNFAIP8* variant 2 (v2) as a p53-regulated gene product that promotes cancer through complex, reciprocal regulatory interactions with p53. We show that *TNFAIP8* v2 may contribute to both carcinogenesis and chemotherapeutic resistance by broadly suppressing p53 activity, thus offsetting p53-dependent tumor suppression.

Results

***TNFAIP8* v1 and v2 are differentially expressed in human cancers.** Recent revisions of the human reference sequence database indicate that *TNFAIP8* (chr5: 118 604 418–118 730 138) has six expression (mRNA) variants. The last exon is common, whereas usage of other exons differs across variants (Supplementary Figure S1). Several reports have shown that *TNFAIP8* is overexpressed in human cancers,^{3–5,8,19–22} yet none of these publications have used methods with adequate specificity to discriminate among

¹Immunity, Inflammation, and Disease Laboratory, National Institute of Environmental Health Sciences, NIH, Research Triangle Park, NC 27709, USA; ²Genome Integrity & Structural Biology Laboratory, National Institute of Environmental Health Sciences, NIH, Research Triangle Park, NC 27709, USA and ³Biostatistics and Computational Biology Laboratory, National Institute of Environmental Health Sciences, NIH, Research Triangle Park, NC 27709, USA

*Corresponding author: JM Lowe or MB Fessler, Immunity, Inflammation and Disease Laboratory, National Institute of Environmental Health Sciences, NIH, 111 T.W. Alexander Drive, P.O. Box 12233, MD D2-01, Research Triangle Park, NC 27709, USA. Tel: 919 541 3967 or 919 541 3701; Fax: 919 541 7593 or 919 541 4133; E-mail: julie.lowe@nih.gov or fesslerm@niehs.nih.gov

⁴These two authors contributed equally to this work.

Abbreviations: BrdU, 5-bromo-2'-deoxyuridine; ChIP-seq, chromatin immunoprecipitation sequencing; DOX, doxorubicin; Gadd45A, growth arrest and DNA damage-inducible 45a; H3K4me1, histone H3 mono-methylation on lysine 4; H3K4me3, histone H3 tri-methylation on lysine 4; H3K27ac, histone H3 acetylation on lysine 27; p53RE, p53 response element; PCNA, proliferating cell nuclear antigen; Scri, cells expressing scrambled shRNA; shRNA, short hairpin RNA; TCGA, The Cancer Genome Atlas; *TNFAIP8*, tumor necrosis factor- α -induced protein 8; TP8i, cells expressing *TNFAIP8* shRNA

Received 18.4.16; revised 02.9.16; accepted 11.10.16; Edited by K Vousden; published online 11.11.16

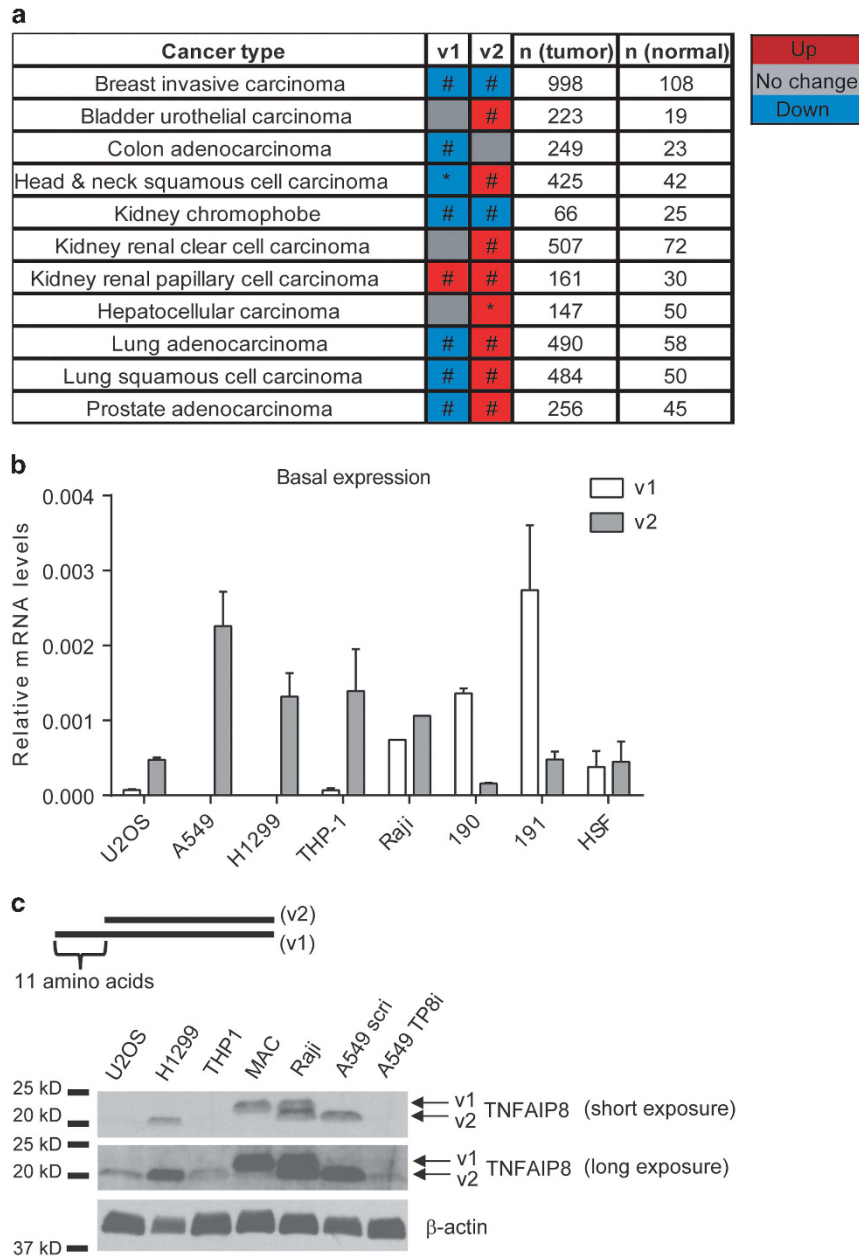


Figure 1 TNFAIP8 variants are differentially expressed in cancer cells. **(a)** A heat map showing significant changes in variant 1 (v1) and variant 2 (v2) expression levels in tumors compared with normal tissue of the same origin. * $P < 0.05$; # $P < 0.01$. Patient-level tumor/normal tissue pairings (same patient) plus unpaired (different patients) samples were analyzed to maximize statistical power. Inpatient paired analysis alone yielded similar results, except that v1 expression was not significantly different in breast carcinoma and lung adenocarcinoma. **(b)** Relative levels of TNFAIP8 v1 and v2 mRNA in the indicated cell lines/types normalized to β -actin. THP-1, acute monocytic leukemia; Raji, B-cell lymphoma; '190' and '191' are primary human macrophages from two donors; HSF, human skin fibroblast. **(c)** Compared with v2, v1 includes additional 11 amino acids. Immunoblot of TNFAIP8 and β -actin (control) was performed in the indicated cell types. 'MAC' refers to primary human macrophages. A549 cells were transduced with either TNFAIP8 shRNA (TP8i) or scrambled control shRNA (scri). Results are representative of three or more independent experiments

TNFAIP8 variants. In order to determine the expression patterns of the variants in human tumors compared with normal tissue, we analyzed cataloged RNA-sequencing (RNA-seq) data from primary human tumor and normal tissue for 11 cancer types in The Cancer Genome Atlas (TCGA)(Figure 1a and Supplementary Figure S2A). v1 and v2 were expressed at appreciable levels in tumor and normal tissue, whereas expression of the other variants was very low or undetectable. v2 was upregulated in nearly all tumors,

whereas v1 was downregulated in most tumors. Taken together, these results indicate that v1 and v2 are differentially regulated in human tumors and reveal that the previously reported increase of TNFAIP8 expression in human cancers is likely due to v2.

v2 is the predominantly expressed TNFAIP8 variant in cancer cell lines. Using specific RT-PCR primers, we measured the relative expression of all TNFAIP8 variants

(v1–v6) in a panel of cell types. Although the relative expression levels of v1 and v2 depend on cell type, these two are the predominantly expressed variants in U2OS (osteosarcoma), A549 (lung cancer), and Raji (B cell lymphoma) cells, as well as human primary macrophages (Supplementary Figures S2B–E). Similar to our findings with human tumors, most of the cancer cell lines we surveyed had much higher levels of v2 than v1 (Figure 1b). There was no detectable v1 in A549 and H1299 cells. On the other hand, Raji cells and human skin fibroblasts have v1~v2, and human macrophages express v1>v2. TNFAIP8 v1 has additional 11 amino acids that v2 lacks, conferring a difference in molecular weight. The relative expression of v1 and v2 proteins (Figure 1c) is consistent with mRNA expression in several cell types. Cytochemistry in A549 cells also shows upregulation of v2 (along with p53) in response to doxorubicin (DOX) and indicates strong nuclear as well as cytoplasmic staining (Supplementary Figure S2F).

TNFAIP8 v2 is induced by DOX in a p53-dependent manner. Nutlin-3, a small-molecule p53 activator, significantly induced v2 along with the classical p53 target p21 in A549 cells (Figure 2a). Given this and our finding that DOX, another well-known p53-activating agent, induces v2, we investigated whether p53 regulates v2 expression. U2OS and A549 cells stably expressing either a scramble (scri) or p53-directed shRNA (p53i)¹⁷ were exposed to DOX. DOX upregulated p53 and induced v2 mRNA in a p53-dependent manner in both lines (Figures 2b–d). Consistent with mRNA, v2 protein was induced in U2OS cells and the induction was blunted by two different p53-directed short hairpin RNAs (shRNAs; Figure 2e). Similarly, expression of v2 and p21 was significantly induced in p53-proficient ('p53+') but not p53-deleted ('p53-') HCT116 colon carcinoma cells (Figure 2f). However, whereas both genes were induced by DOX within 12 h in p53+ HCT116 cells and U2OS cells, only p21 was induced by 6 h, indicating that v2 induction may occur later than p21 (Figure 2g). In the absence of DOX, no difference in v2 expression was detected between p53+ and p53- HCT116 cells or between p53-silenced and control U2OS cells, suggesting no requirement for p53 in basal expression of v2 in cancer cells (Figures 2e–g).

p53 binds to the TNFAIP8 gene. In order to characterize p53 regulation of DOX-induced v2, we searched p53 chromatin immunoprecipitation sequencing (ChIP-seq) data from U2OS cells treated with DOX¹⁷ for p53 binding near TNFAIP8. A large peak was found in the first intron of v2 distant from the v1 or v2 start sites (Figure 3a). A scan for potential p53 response elements (REs)^{23,24} confirmed that this site encompasses a p53RE predicted to be functional¹⁶ (coordinates are chr5: 119 323 861–119 323 880 in latest human genome annotation, 'GRCh38/hg38', Figure 3a). Binding of p53 to this site was validated with p53 ChIP-PCR in U2OS cells, with binding to the p21 promoter region serving as a positive control (Figure 3b). Analysis of published p53 ChIP-seq data sets revealed that, remarkably, p53 binds to the same TNFAIP8 intronic region in a very wide range of cell types in response to various p53-activating agents (Supplementary Table S1).

Having identified a p53-binding site, we further characterized p53 regulation of TNFAIP8 using U2OS cells as a model system. We cloned a ~600 bp region encompassing the p53RE upstream of a luciferase reporter. An empty vector, the v2 p53RE vector, or a positive control vector with confirmed functional p53REs, each upstream of a luciferase reporter construct, were individually transfected into U2OS cells stably expressing either a scrambled or p53-directed shRNA (Figure 3c). Treatment with DOX significantly enhanced luciferase activity (v2 p53RE and p53+ only) in scramble shRNA cells. Both basal and DOX-induced luciferase were significantly reduced in p53-depleted cells. These results confirm that the p53RE in the v2 intron is functional as this region confers p53-dependent transactivation ability.

The intronic p53-binding region in TNFAIP8 is an enhancer. The p53-binding region lies within the first intron of v2. However, it is ~50 kb downstream from the v2 promoter region and ~30 kb upstream from the v1 promoter region, suggesting that it may possibly be an intragenic enhancer. To address this possibility, we analyzed it for enhancer-like chromatin marks. Chromatin marks characteristic of enhancers include high histone H3 mono-methylation on lysine 4 ('H3K4me1'), high histone H3 acetylation on lysine 27 ('H3K27ac') and low histone H3 tri-methylation on lysine 4 ('H3K4me3'). These contrast with characteristic promoter chromatin marks (low H3K4me1, high H3K27ac, high H3K4me3).²⁵ Using ChIP-PCR, we measured these marks in U2OS cells in the intronic p53-binding region and, for comparison purposes, in the v2 promoter region (V2P). As shown in Figure 3d, regardless of DOX treatment, v2 p53RE has significantly higher H3K4me1 and lower H3K4me3 compared with V2P. Both sites show moderate levels of H3K27ac. Thus, the v2 p53RE region has marks characteristic of an enhancer.

To further validate v2 p53RE as an intragenic enhancer, three-dimensional chromatin looping assays using EcoRI restriction of fixed chromatin followed by PCR using primers designed to survey the region were performed to test whether v2 p53RE physically interacts with V2P despite being ~50 kb removed. Activated p53 has been shown to act on preexisting chromatin loops.²⁵ The primer pair '1/4' yielded significant amplification (Figure 3e), indicating ligation between restricted ends of sites 1 and 4 and the physical interaction between the v2 promoter and the v2 p53RE region through chromatin looping. These data, together with the presence of enhancer-like chromatin marks and transactivation capacity of v2 p53RE, suggest that p53 regulates DOX-induced v2 expression through binding to the v2 p53RE intragenic enhancer region.

TNFAIP8 v2 silencing induces widespread p53 binding and p53 target induction. Given our finding that v2 is upregulated across several human cancers and that basal v2 expression in cancer cell lines is p53 independent, we hypothesized that v2 might promote cancer cell survival through suppressing p53 activities. Several prior examples of reciprocal p53 target regulatory loops have been described.²⁶ In order to address this, we transiently expressed TNFAIP8-directed shRNA ('TP8i') versus scramble shRNA ('scri') in

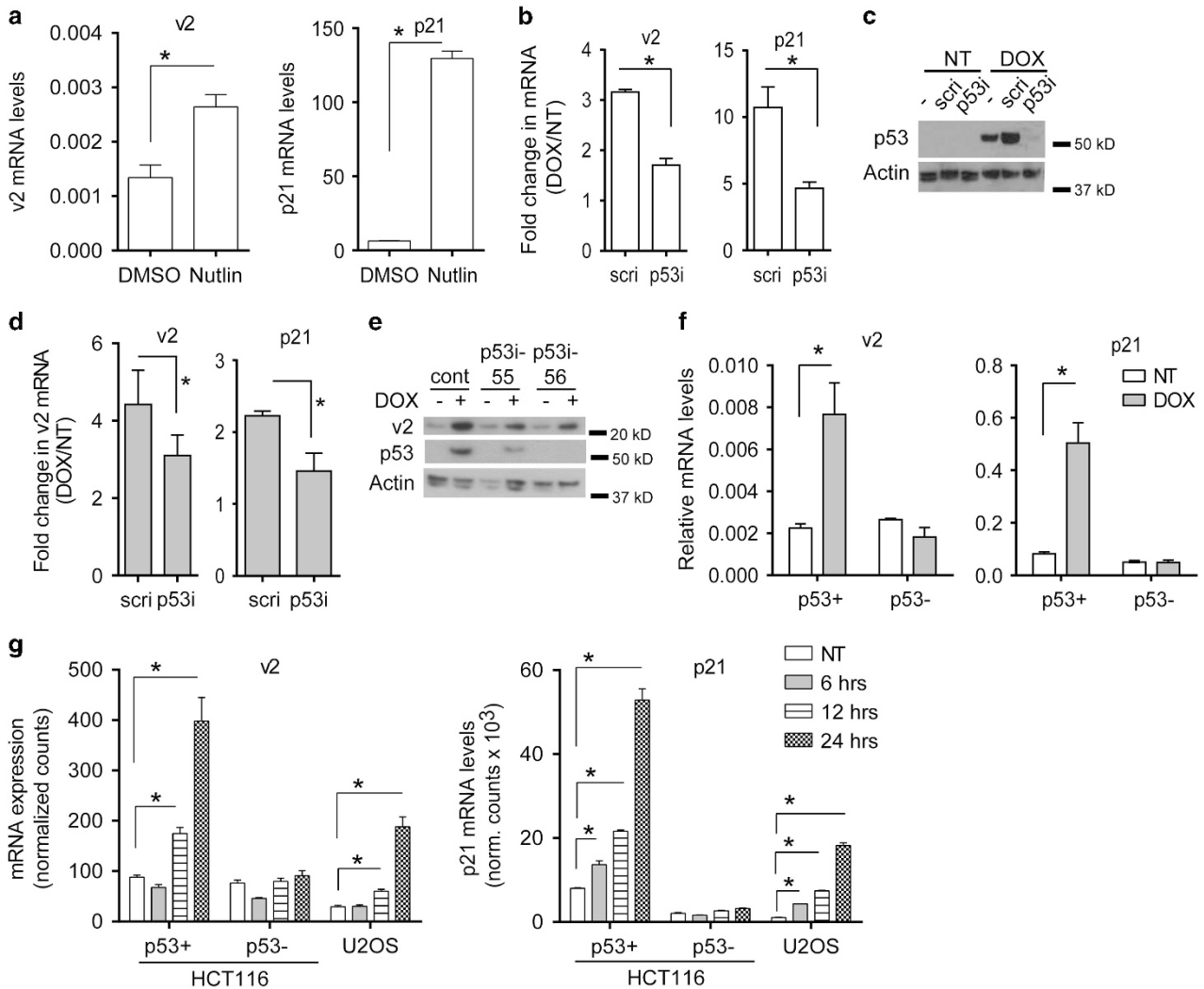


Figure 2 p53 regulates DOX-induced TNFAIP8 v2. (a) v2 and p21 mRNA expression in A549 cells after nutlin-3 or DMSO (vehicle) treatment (24 h). (b) v2 and p21 expression after DOX treatment in A549 cells stably expressing scramble shRNA ('scri') or p53 shRNA ('p53i'). Fold change is displayed as the ratio of DOX-treated over nontreated (NT) cells. (c) Immunoblotting of p53 and actin (loading control) in parental ('-'), scri, and p53i A549 cells following no treatment (NT) or DOX. (d) DOX-induced v2 mRNA expression in U2OS cells stably expressing scri or p53i. (e) v2 and p53 protein levels are shown in untreated and DOX-treated U2OS cells stably expressing scramble control shRNA ('cont') or two different p53-directed shRNAs ('p53i-55' and 'p53i-56'). (f) v2 and p21 mRNA expression in untreated or DOX-treated p53-proficient and p53-null HCT116 cells. (g) v2 and p21 mRNA expression was measured with Nanostring technology in indicated cell types, untreated ('NT') or treated with DOX for durations shown. Results are representative of three or more independent experiments. * $P < 0.05$

(v1-null) A549 cells (Figure 4a). Unexpectedly, we found that p53 protein levels in nuclear extracts and whole-cell lysates were decreased in v2-depleted cells (Figure 4b). We reasoned that one possible explanation might be that p53 was relocalized to chromatin and therefore insoluble in the extraction buffer. To address this, we isolated chromatin-bound nuclear protein and, using specific antibodies, measured both total p53 and acetylated p53, as acetylation is associated with p53 activation and enhanced binding to p53REs.²⁷ Both total and acetylated p53 were indeed increased in the chromatin-bound nuclear fraction in v2-depleted cells, suggesting that v2 silencing regulates p53 by promoting its acetylation and localization to chromatin (Figure 4c). ChIP assays also revealed that p53 enrichment at the promoter regions of multiple established p53 target

genes was significantly greater in v2-depleted cells than in control cells (Figure 4d).

We verified that some target genes displaying increased p53 binding also had increased expression in TP8i cells (Figures 4e and f). A second TNFAIP8-directed shRNA, which depleted v2 by ~37%, resulted in similar expression changes (Supplementary Figures S3A and B). Not all genes displaying increased p53 binding upon v2 silencing had a corresponding change in mRNA expression (e.g., MDM2, DDB2; data not shown). This is consistent with past reports that mRNA expression of p53 target genes may be regulated by mechanisms beyond binding.¹⁷ As v2 depletion led to enhanced p53 activity, we predicted that overexpression of v2 may inhibit p53 activity. v2 overexpression indeed decreased p53 binding to several targets (Figures 4g and h).

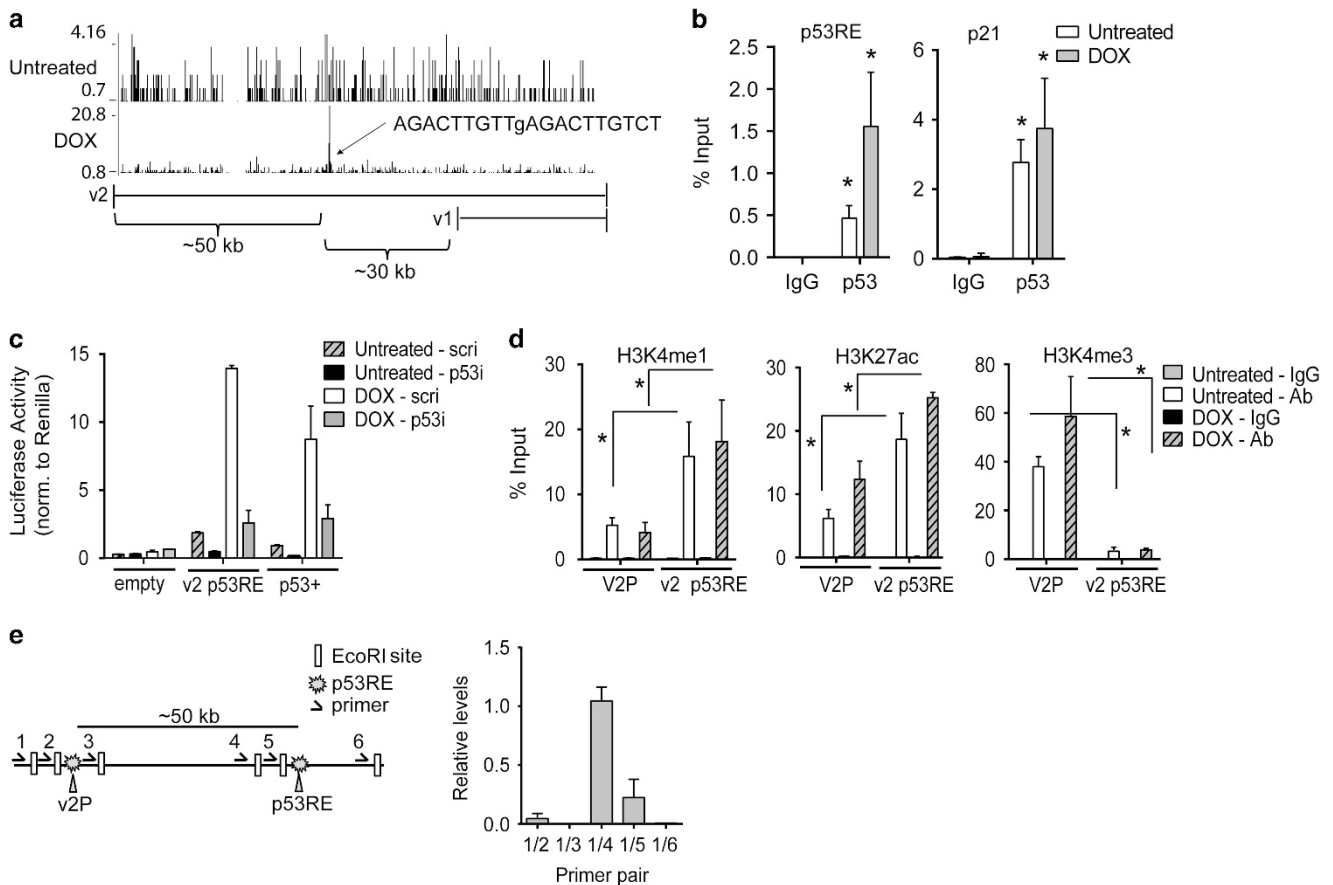


Figure 3 p53 binds to an intragenic enhancer region in *TNFAIP8*. (a) ChIP-seq analysis in U2OS cells untreated or treated with DOX shows p53 enrichment in the v2 intronic region of *TNFAIP8*. v1 and v2 genomic locations are shown below (exons depicted as vertical ticks). The p53 binding peak is 50 kb downstream and 30 kb upstream from the v2 and v1 transcriptional start sites, respectively. ‘p53 Scan’ software analysis reveals a predicted functional p53 response element (RE), as indicated. Lowercase letter indicates mismatches compared with p53RE consensus (RRRCWWGYYnRRRCWWGYYY).¹⁶ (b) Validation of p53 binding to v2 intronic region was tested by p53 ChIP-PCR (or IgG control) in untreated and DOX-treated U2OS cells (depicted as % of total input DNA). p53 binding to the p21 promoter is shown as positive control. (c) Luciferase activity was measured in untreated or DOX-treated U2OS cells stably expressing scramble (‘scri’) or p53-directed shRNA (‘p53i’) and transfected with firefly luciferase reporter constructs without (‘empty’) or with a 600 bp region encompassing the intronic p53RE region. ‘p53+’ is a p53RE-driven luciferase construct (positive control). (d) H3K4me1, H3K27ac, and H3K4me3 ChIP-PCR is shown for the intronic p53RE region (‘v2 p53RE’) and the v2 promoter (‘V2P’) in untreated and DOX-treated U2OS cells (‘Ab’ (antibody)). (e) Schematic showing the 6 EcoRI sites that were used for a three-dimensional chromosome looping assay, as they relate to the v2 promoter region and the intronic p53RE. PCR was performed using the indicated primer pairs in untreated U2OS cells. Results are representative of three or more independent experiments. * $P < 0.05$

Collectively, these findings suggest that TNFAIP8 v2 exerts complex regulation of p53 function in cancer cells, where it restrains p53 from activating select nuclear genes.

TNFAIP8 v2 depletion inhibits DNA synthesis and leads to cell cycle arrest. To date, no study has defined variant-specific functions for TNFAIP8 in cancer. As we found that v2 was overexpressed in cancers and appears to suppress p53, we hypothesized that v2 might promote cancer cell growth. To address this, v2 silencing was performed in A549 cells stably expressing either p53-directed shRNA (‘p53i’) or a scramble shRNA (‘p53+’)(Figure 5a) and DNA synthesis examined using 5-bromo-2'-deoxyuridine (BrdU) incorporation. As shown in Figure 5b, p53+ and p53i cells with scramble shRNA displayed considerable BrdU staining intensity. In stark contrast, v2-depleted p53+ cells showed low BrdU staining. Quantification of BrdU intensity revealed a significant difference between TP8i and control cells in both

the p53+ and p53i background (Figure 5c). As the effect of v2 depletion on DNA synthesis was less in p53i than p53+ cells (37% versus 68% reduction; $P < 0.05$), we conclude that DNA synthesis arrest in TP8i cells is at least partially p53 dependent, but can nonetheless proceed in p53-deficient cells. Interestingly, there was no significant difference in the percentage of TP8i and Scri cells that were BrdU positive (Supplementary Figure S3C), indicating that DNA synthesis is initiated in v2-depleted cells but unable to progress.

Given that v2-depleted cells displayed defective DNA synthesis, we next analyzed the cell cycle profile. Cell cycle analysis using 7-aminoactinomycin D (7AAD) revealed a stalling in S phase of v2-depleted cells compared with controls (Figure 5d and Supplementary Figure S3D). Despite our finding that the DNA synthesis defect caused by v2 depletion occurs in both p53+ and p53i cells, v2-depleted p53i cells did not arrest in the S phase, indicating a requirement for p53 in the S-phase arrest (Figure 5d).

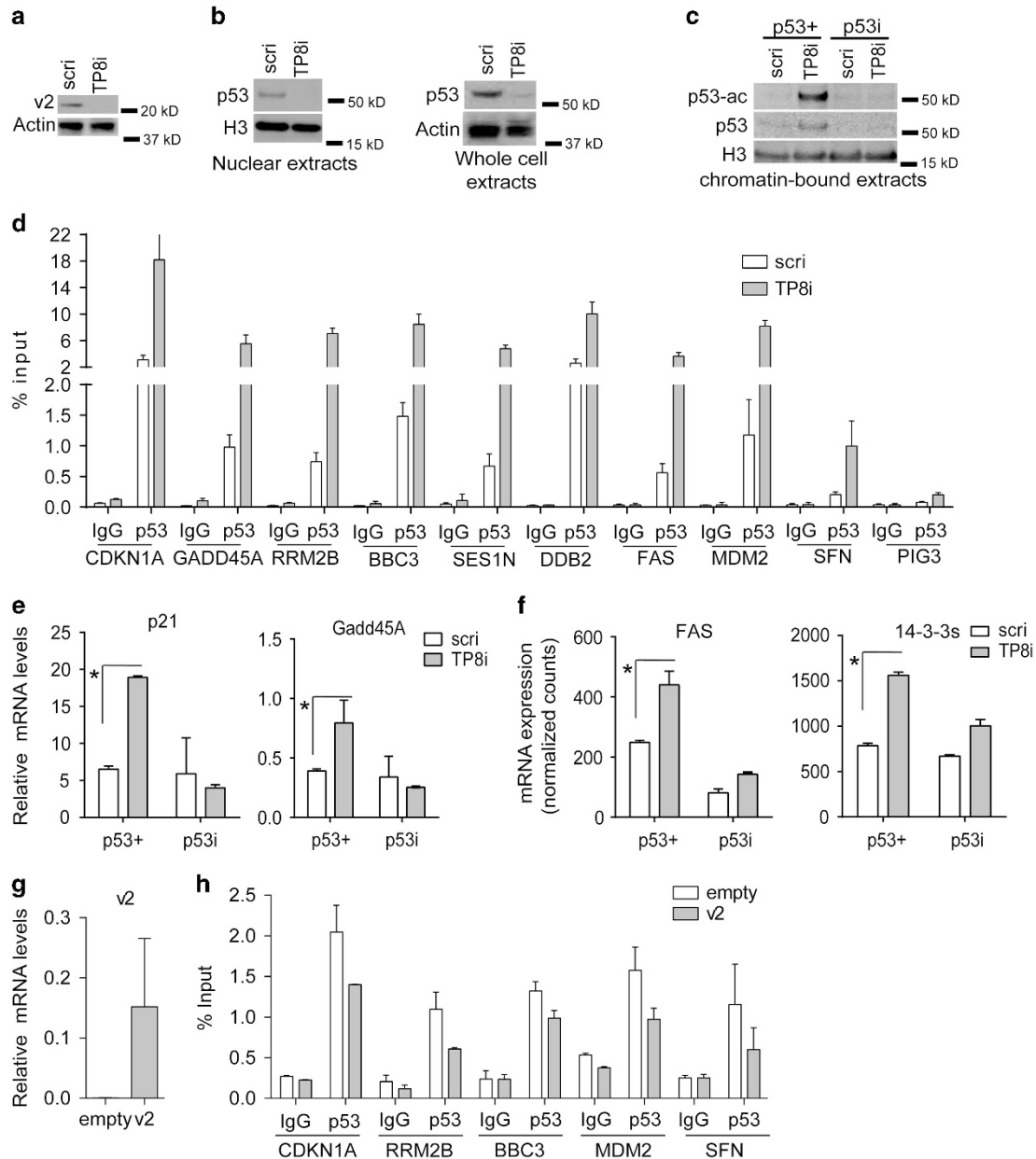


Figure 4 TNFAIP8 v2 depletion induces p53 binding and p53 target expression. (a) Immunoblot of v2 and actin (control) in whole-cell lysates of A549 cells treated with TNFAIP8 (TP8i) or scrambled (scri) shRNA. (b) Immunoblot of p53 from nuclear and whole-cell extracts of cells under indicated treatments. (c) Immunoblot of acetylated p53-K382 (p53-ac) and total p53 in chromatin-bound nuclear extracts of p53+ or p53-silenced A549 cells treated with scri or TP8i. Histone 3 (H3) and actin are loading controls. (d) p53 CHIP-PCR of promoter regions of indicated target genes in TP8i and scri cells. IgG serves as negative control. (e and f) mRNA expression of p21 and Gadd45a (RT-PCR) (e) and FAS and 14-3-3 σ (Nanostring) (f) was measured in p53+ or p53-silenced A549 cells treated with scri or TP8i. (g) v2 mRNA expression (normalized to *GusB*) and (h) p53 binding to the indicated target genes was measured with RT-PCR and ChIP-PCR, respectively, in A549 cells transiently transfected with an empty vector ('empty') or a v2 expression vector ('v2'). Results are representative of three or more independent experiments. * $P < 0.05$

GADD45A and *CDKN1A* (p21), both of which regulate cell cycle arrest^{28,29} and are induced by p53, were significantly upregulated in v2-depleted cells compared with controls in a p53+, but not p53i, background (Figure 4d and Supplementary Figure S3B), suggesting they may contribute to the p53-dependent S-phase arrest in v2-depleted cells. On the other hand, proliferating cell nuclear antigen (PCNA), which is required for progression of DNA replication,³⁰ was significantly reduced in TP8i cells in both the p53+ and p53i settings

(Figure 5e). As PCNA is dispensable for initiation of DNA replication but required for progression,³⁰ our finding that PCNA is decreased in v2-depleted cells irrespective of p53 status is consistent with our finding of a defect in the progression but not initiation of DNA synthesis in both p53+ and p53i v2-depleted cells (Figures 5b and c).

Cyclins D1, E1, and E2 are all required for transition from G1 to S phase, after which the expression of these cyclins must be decreased to maintain the proliferation signal and progress

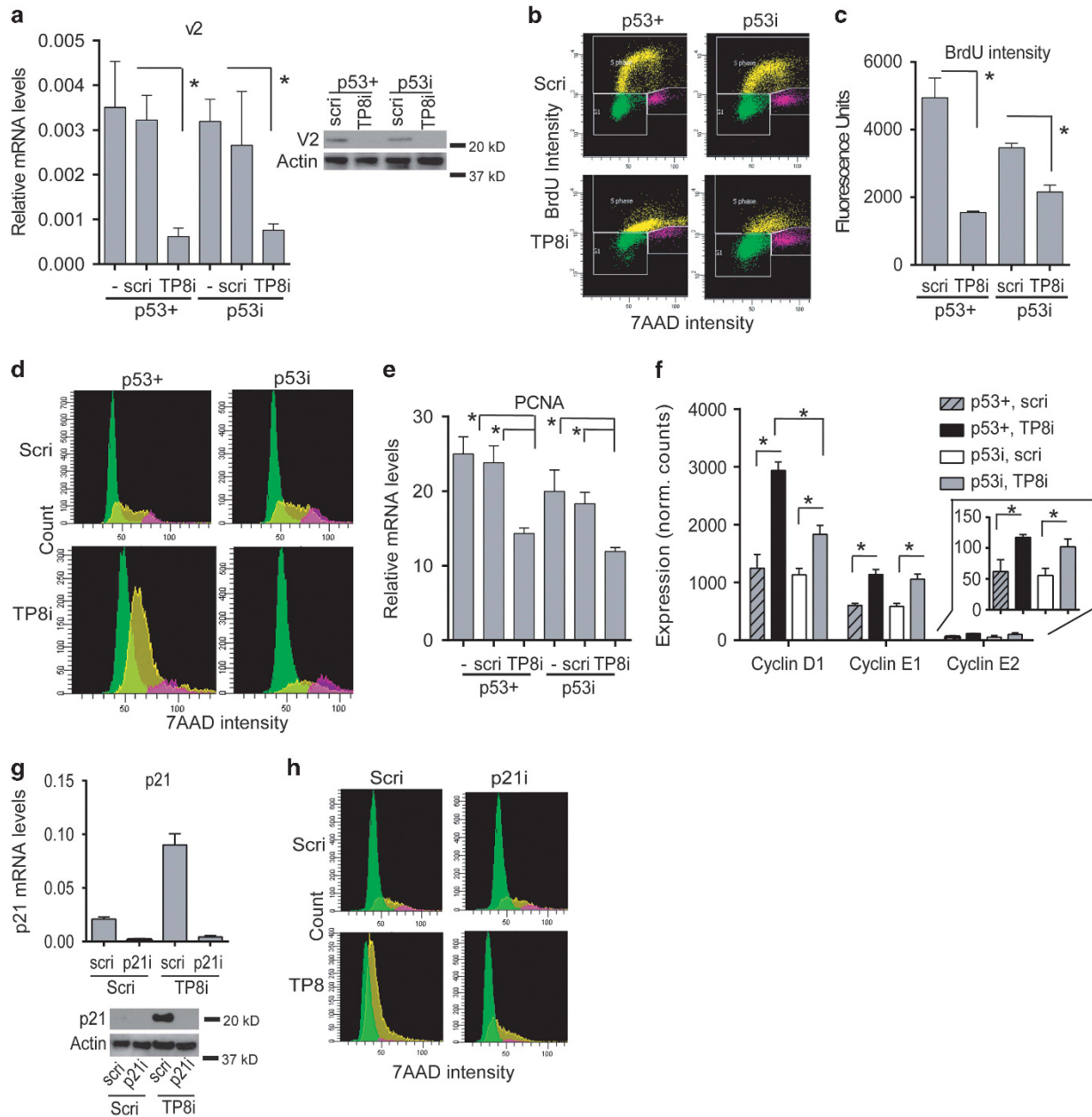


Figure 5 TNFAIP8 v2 depletion stalls DNA replication and induces p53-dependent cell cycle arrest. (a) TNFAIP8 v2 mRNA levels were quantified in p53+ and p53-silenced (p53i) A549 cells untransduced (‘-’) or transduced with scramble (‘scri’) or TNFAIP8-directed (‘TP8i’) shRNA. At right, an immunoblot of v2 under the same conditions is shown. (b) 5-Bromo-2'-deoxyuridine (BrdU) incorporation and 7AAD staining were quantified using flow cytometry in p53+ and p53i A549 cells transduced with scri or TP8i shRNA. BrdU+ cells (S phase), yellow; G1, green; G2, purple. (c) Quantification of BrdU intensity of cells in (b). (d) Cell cycle profile based on 7AAD staining of cells in (a). G2-phase cells (purple) are defined as cells with double the nuclear 7AAD stain intensity compared with G1-phase cells (green). S-phase cells are BrdU+ (yellow). (e and f) mRNA levels of PCNA (RT-PCR) (e) and cyclins D1, E1, and E2 (Nanostring) (f) of cells under indicated treatments. (g) p21 quantified by RT-PCR and immunoblot in p53+ A549 cells transduced with either scri or TP8i shRNA, followed by transfection of scramble (‘scri’) or p21 (‘p21i’) siRNA. (h) Cell cycle analysis of cells described in (g). Results are representative of three or more independent experiments. * $P < 0.05$

through S phase.^{31–33} We hypothesized that expression of these cyclins might be increased in v2-depleted cells given the observed S-phase arrest (Figure 5d). Consistent with our prediction, cyclins D1, E1, and E2 were all significantly increased in v2-depleted cells (Figure 5f). Unlike the case for cyclins E1 and E2, cyclin D1 induction in TP8i cells appeared to be p53 dependent. This finding is consistent with previous

reports describing p53 enhancement of cyclin D1 expression and subsequent growth arrest.^{34,35}

To test whether the S-phase arrest induced by v2 depletion was specific for A549 cells, we performed similar experiments in U2OS, MCF-7 (breast cancer), and HCT116 cells, all of which, like A549 cells, predominantly express v2 and little v1. As with A549 cells, v2 depletion in all cell lines significantly

upregulated p21 (Supplementary Figures S4A–C) and impaired proliferation (not depicted). However, the percentage of cells in G1 was significantly increased in v2-depleted U2OS and MCF-7 cells, whereas v2-depleted HCT116 cells exhibited an increase in G2/M, indicating an arrest in G1 and G2/M, respectively (Supplementary Figures S4D–F and S5). Taken together, all cancer cell lines surveyed displayed upregulation of p21 with v2 depletion, but, interestingly, exhibited a variety of types of cell cycle arrest.

Cell cycle arrest in v2-depleted cells is primarily due to p21. Our results in A549 cells indicated that v2 depletion leads to defective DNA replication progression, potentially through downregulated PCNA and S-phase stalling. However, in an effort to identify gene networks in a more unbiased manner that might account for these findings, gene expression was profiled in A549 cells using Nanostring technology. Of 770 genes in the Nanostring PanCancer Codeset, 221 (28.7%) were significantly altered in expression in response to v2 silencing. Ingenuity Pathway Analysis revealed that the highest scoring network of genes with significant expression changes upon v2 silencing in p53+ cells was that associated with cell proliferation and cell cycle, and that this network centered upon *CDKN1A* (i.e., p21) (Supplementary Figure S6). In order to address whether p21 orchestrates the p53-dependent cell cycle arrest induced by v2 depletion, we introduced scrambled or pooled p21-directed siRNA into TP8i and scri, p53+ A549 cells (Figure 5g). p21 silencing prevented the S-phase arrest in v2-depleted cells (Figure 5h), confirming p21 as a major p53-responsive driver of the defective cell growth of TP8i cells.

TNFAIP8 v2 depletion enhances damage-induced apoptosis. We next evaluated the impact of v2 on the response of cancer cells to chemotherapeutic challenge. As shown in Figures 6a and b, DOX induced a dramatic, nearly ninefold higher frequency of apoptosis (51% versus 6%) in v2-depleted cells than in controls. The increased apoptosis appears to be at least partially p53 dependent (Figure 6b). Similar results were seen with the nongenotoxic agent staurosporine³⁶ (Figure 6c and Supplementary Figure S7). TP8i cells also showed significantly higher activation of the executioner caspases 3/7 in response to both DOX and staurosporine in a p53+, but not p53i, background (Figure 6d). Depletion of v2 thus sensitizes cancer cells to p53-dependent DOX- and staurosporine-induced apoptosis. These results suggest that TNFAIP8 v2 is an anti-apoptotic regulator in response to chemotherapeutics, attenuating chemotherapeutic efficacy by reducing p53-dependent death.

Discussion

We identify TNFAIP8 v2 as a gene product that is upregulated in a wide array of human cancers and show that, in the absence of exogenous stress, TNFAIP8 v2 engages in complex, reciprocal regulatory interactions with p53 that may contribute to both tumorigenesis and chemotherapeutic resistance of tumors (Figure 7). Our v2-silencing studies in steady-state A549 cells suggest that v2 acts to support DNA synthesis and may repress p53-dependent cell cycle arrest by

suppressing acetylation of p53 and induction of p53 targets, in particular, p21. Among defective DNA synthesis and cell cycle arrest (the major outcomes of v2 silencing in steady-state A549 cells), only the former is substantially p53 independent. Given that replication stress is a well-known trigger for p53 activation,³⁷ we speculate that the sequence of events triggered by v2 silencing in A549 cells may be as follows: failed DNA synthesis, p53 activation, and then p53-dependent cell cycle arrest. On the other hand, v2 depletion in U2OS, HCT116, and MCF-7 cells does not cause DNA synthesis failure, but instead induces G1 or G2/M arrest, thus indicating that the mechanism of v2 in cancer is cell-type specific. Finally, in the context of genotoxic stress, such as after cancer chemotherapeutic exposure, p53 is increased and induces v2 through binding to an intragenic enhancer region. In turn, v2 negatively feeds back upon p53, suppressing p53-mediated apoptosis and promoting tumor resistance.

The precise molecular mechanisms by which v2 regulates p53 activation and PCNA induction remain unclear, and warrant future investigation. Of interest, TNFAIP8 has been proposed to be a scaffolding protein, and both p53 and PCNA were previously identified as potential TNFAIP8-binding partners.⁴ It is thus intriguing to consider the possibility that v2 binding may possibly regulate access of acetylases and/or deacetylases to p53. TNFAIP8 could also conceivably regulate the activity of a signaling protein or transcription factor (other than p53 (Figure 5e)) that regulates PCNA expression.

Our data suggest that v2 may be regulated by transcription factors other than p53. Induction of TNFAIP8 by TNF α appears to be dependent on NF- κ B.⁹ Regulation of *TNFAIP8* by factors other than p53 may be especially important in cancer cells as it is well known that a large portion of tumors have mutated p53.³⁸ As NF- κ B is constitutively activated in many cancers,³⁹ it may drive v2 expression in cancer cells with mutated p53. On the other hand, some cancer-associated p53 mutants exhibit alterations in target gene regulation,^{24,38} thus, it is possible that mutated p53 may have an enhanced ability to induce v2 in tumors. Regardless, we show that v2 can influence responses to chemotherapeutic agents even under conditions of reduced p53 and that v2 silencing arrests DNA replication even in cancer cells depleted of p53.

Our findings point to the presence of a negative feedback loop between TNFAIP8 v2 and p53 in the context of stress and DNA damage signaling. The feedback of TNFAIP8 upon p53 could be similar to the p53-Wip1 feedback loop⁴⁰ and serve as a mechanism by which p53 signaling is brought back to prestress levels when damage is repaired. Our findings that v2 is a late-responding p53 target gene (Figure 2g) fit with this hypothesis that v2 could have a role in homeostatic regulation. We speculate that elevated v2 expression supports cancer cell proliferation and survival and that it may also promote chemotherapy resistance.

Therapeutic inhibition of v2 in conjunction with DNA-damaging anticancer drugs used in the clinic might provide synergy by removing restraint upon p53 tumor suppressive function. We speculate that v2 suppression of p53 signaling in noncancerous cells (harboring wild-type p53) may also protect healthy tissue during chemotherapy.⁴¹ Thus, targeting v2 inhibition specifically to cancer cells, for example,

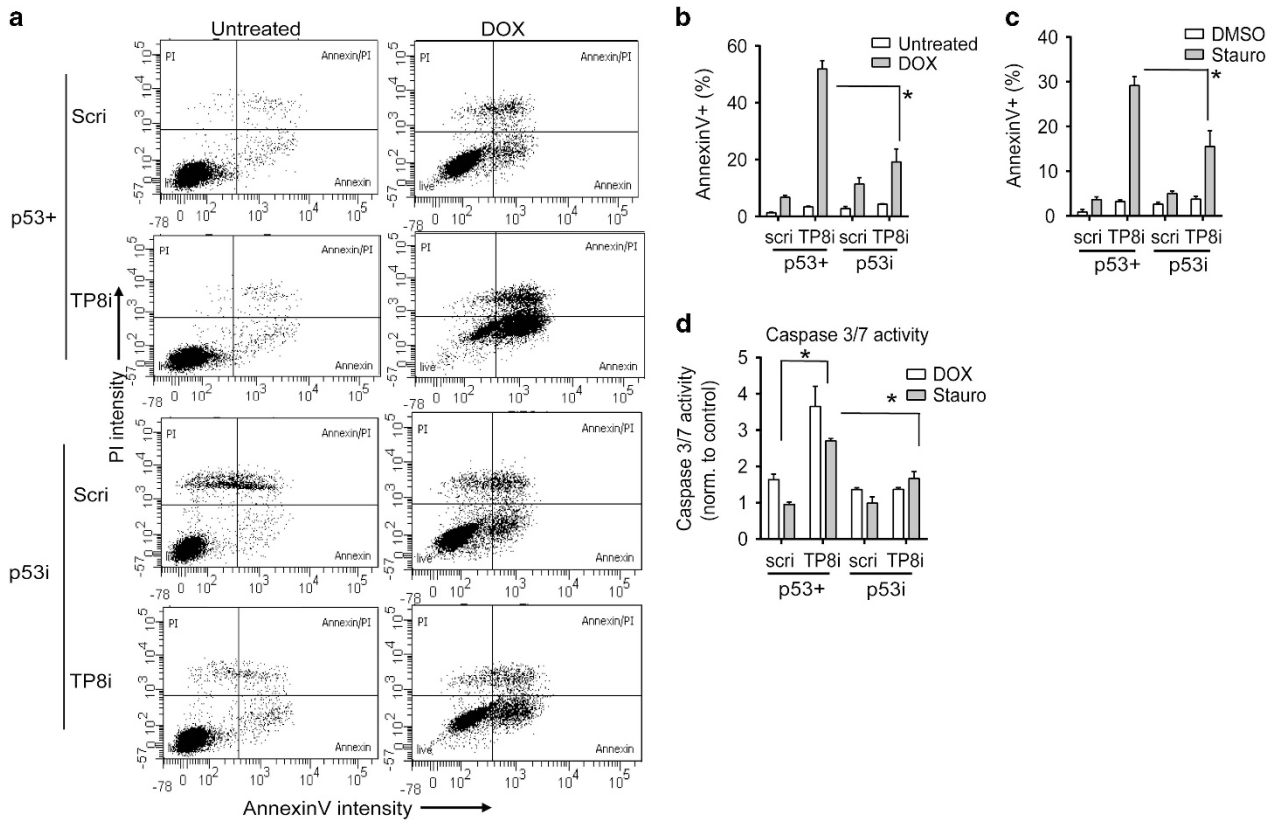


Figure 6 TNFAIP8 v2 depletion enhances damage-induced apoptosis. (a) Annexin V and propidium iodide (PI) staining were quantified by flow cytometry in p53+ and p53i A549 cells transduced with a scramble ('Scri') or TNFAIP8-directed ('TP8i') shRNA and untreated or treated with DOX. (b and c) The percentage of Annexin V+ cells was quantified in untreated and DOX-treated cells (b), and in DMSO-treated cells (vehicle control) and staurosporine ('Stauro')-treated cells (c). (d) The fold change in caspase 3/7 activity is shown in the cells described in (b and c) after DOX or Stauro treatment. DOX and Stauro values are normalized to untreated or DMSO-treated values, respectively. Results are representative of three or more independent experiments. * $P < 0.05$

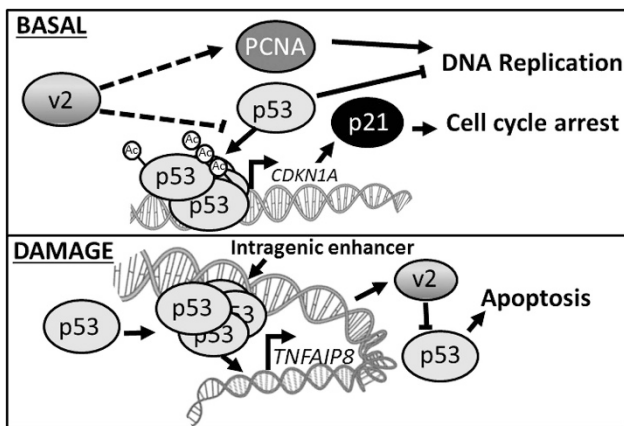


Figure 7 Proposed scheme of interactions of TNFAIP8 v2 with p53 in cancer. Under basal conditions in A549 cancer cells, v2 promotes DNA replication, possibly by maintaining PCNA levels, and inhibits cell cycle arrest through restraining p53-dependent expression of p53 target genes including p21. Failed downregulation of cyclins may also contribute to S-phase stalling. In response to DNA damage (e.g., DOX), p53 promotes v2 induction. v2, in turn, suppresses p53-dependent pro-apoptotic responses. In this manner, basal overexpression of TNFAIP8 v2 may promote tumorigenesis (by facilitating DNA replication and preventing cell cycle arrest), whereas p53-induced v2 in the setting of DNA-damaging agents may also promote resistance to cancer therapy (by suppressing apoptosis)

with nanocarriers, antibody–drug conjugates, or other approaches,^{42,43} may maintain v2/p53-dependent protection of normal cells while sensitizing tumor cells to DNA-damaging drugs. Furthermore, as sensitization of cancer cells to therapy by v2 depletion appears to require p53, inhibition of v2 along with administration of small molecules that activate wild-type p53 or revert mutant p53 to function like wild-type p53 (e.g., nutlin-3, RITA, PK7088^{44–46}) may also be beneficial for cancer treatment.

In summary, we identify variant 2 of *TNFAIP8* as an oncogenic gene product that appears to be required for several hallmark features of cancer cells, including sustained proliferative signaling, evasion of growth suppressors, and resistance to cell death.⁴⁷ Mechanistically, our results highlight that v2 participates in reciprocal regulation with p53 and exerts broad suppression of p53 functions. We propose that TNFAIP8 v2 may be a fruitful target for therapeutic development in cancer.

Materials and Methods

Reagents and cell lines. U2OS, A549, THP-1, HCT-116, and Raji cell lines were cultured as described by American Tissue Culture Collection (Manassas, VA, USA). Human monocyte-derived macrophages were cultured as previously described, in accordance with a NIEHS IRB-approved protocol.⁴⁸ Human skin

fibroblasts were cultured as previously described.⁴⁹ DOX, staurosporine, and nutlin-3 (Sigma-Aldrich, St. Louis, MO, USA) were used at 0.3 μ g/ml, 2.5 μ M, or 10 μ M, respectively.

Lentiviral transduction and plasmid transfection. A549 cells stably expressing scramble or p53-directed shRNA were established as previously described.¹⁷ Cells were transduced with either lentiviral scramble shRNA or a validated TNFAIP8-directed shRNA (Cat. no. SHCLND-NM_014350, TRC: TRCN0000116159, Sigma-Aldrich; 24 h). After 48 h, the cells were treated or assayed. For v2 overexpression, empty (pCMV-entry, Origene, Rockville, MD, USA) or v2 expression vector (RC220669, Origene) were transiently transfected using Lipofectamine 3000 (ThermoFisher Scientific, Waltham, MA, USA; 24 h).

TCGA data analysis. The results are in whole or part based upon data generated by the TCGA Research Network: <http://cancergenome.nih.gov/>. Isoform-level normalized RSEM scores for TNFAIP8 transcripts (uc003ksi, uc003ksg) available as of 1 October 2014 were extracted from bulk download data files: <https://tcga-data.nci.nih.gov/tcga/>. Transcript quantification scores were collected (number of inpatient tumor/normal tissue-matched samples): bladder urothelial carcinoma ($N=19$), lung adenocarcinoma ($N=57$), renal papillary cell carcinoma ($N=30$), kidney chromophobe cancer ($N=25$), prostate adenocarcinoma ($N=45$), lung squamous cell carcinoma ($N=50$), renal clear cell carcinoma ($N=72$), head and neck squamous cell carcinoma ($N=40$), breast cancer ($N=110$), hepatocellular carcinoma ($N=50$), and colon adenocarcinoma ($N=22$).

Real-time PCR. RNA was reverse transcribed using the cDNA Reverse transcription kit (Applied Biosystems, Waltham, MA, USA) and used as template for SYBR green and TaqMan expression assays according to the manufacturer's guidelines (Applied Biosystems). Primers and primer/probe sets are described in Supplementary Table S1.

ChIP-seq and PCR. The p53 ChIP-seq and PCR were as previously described¹⁷ (Supplementary Table S2). Briefly, the chromatin was fixed (1% formaldehyde for 10 min, then neutralized with 0.125 mM glycine), and nuclei were harvested in Farnham lysis buffer (5 mM PIPES, pH 8.0, 85 mM KCl, 0.5% NP-40). The chromatin was extracted with RIPA buffer (1% NP-40, 0.5% sodium deoxycholate, 0.1% SDS in PBS) and sheared by sonication (three 15 min cycles of 30 s on, 30 s off). DNA was isolated after immunoprecipitation with either a mouse IgG (negative control, Santa Cruz) or p53 antibody (DO-1, Santa Cruz, Dallas, TX, USA). For ChIP-PCR, specific primers (Supplementary Table S2) were used in SYBR green PCR assays according to the manufacturers protocol (Applied Biosystems). Sequencing (ChIP-seq) was performed as previously described.¹⁷

Immunoblotting and immunofluorescence. Immunofluorescence and immunoblotting was performed as previously described.⁴⁸ Whole-cell extracts, nuclear extracts, and chromatin-bound extracts were isolated with RIPA buffer (50 mM Tris, pH 8, 150 mM NaCl, 1% NP-40, 0.1% SDS, 0.5% deoxycholic acid), the NE-PER kit (ThermoFisher Scientific), and the subcellular protein fractionation kit for cultured cells (ThermoFisher Scientific), respectively. For immunofluorescence, cells were cultured on coverslips and fixed and permeabilized with 4% formaldehyde and 0.1% Triton X-100, followed by probing with antibodies for proteins of interest. Antibodies are in the Supplementary Information.

Promoter cloning and reporter assays. Cloning into the pGL4.26 firefly luciferase reporter vector (Promega, Madison, WI, USA) and assay of *Renilla* luciferase-normalized (pRL-SV40 *Renilla* luciferase control vector, Promega) activity were performed as previously reported with the dual-luciferase reporter assay per the manufacturer's protocol (Promega).⁵⁰ Cloning and primer details are described in Supplementary Information.

Three-dimensional chromatin capture assay (3C assay). An established protocol was followed.⁵¹ Briefly, chromatin was crosslinked with formaldehyde, neutralized with glycine, harvested with lysis buffer (10 mM Tris-HCl (pH 8.0), 10 mM NaCl, 0.2% NP-40,) digested with *EcoRI*, ligated at 3 ng/ μ l DNA with T4 ligase, and analyzed by PCR (Supplementary Table S1).

BrdU assay and cell cycle analysis. Cells were pulsed with BrdU (10 μ M, 30 min) and processed according to the manufacturer (BD Biosciences/Pharmingen, San Jose, CA, USA). Fluorescence was measured with a LSRII

Flow Cytometer (Becton Dickinson, Franklin Lakes, NJ, USA) after gating on single cells.

Annexin V and caspase activation assays. The manufacturer's protocols were followed: Annexin V-FITC kit (Cat. no. 4830-01-K, Trevigen, Gaithersburg, MD, USA) and Caspase-Glo 3/7 assay (Cat. no. G8090, Promega).

Nanostring assay. Expression of genes in the PanCancer pathways panel and a custom codeset were measured as per the manufacturer (NanoString Technologies, Seattle, WA, USA) with nCounter Digital Analyzer and nSolver (v2.5) software. Additional details regarding analysis are in the Supplementary Information.

Statistical analysis. Data were graphed and analyzed with GraphPad Prism software (La Jolla, CA, USA). Student's *t*-test was used for statistical analysis. $P < 0.05$ was defined as significant.

Conflict of Interest

The authors declare no conflict of interest.

Acknowledgements. We thank NIEHS core facilities: molecular genomics, viral vector, flow cytometry, microscopy, and the Clinical Research Unit. This research was supported by the Intramural Research Program of the National Institutes of Health, NIEHS (Z01 ES102005, Z01-ES065079).

- Kumar D, Whiteside TL, Kasid U. Identification of a novel tumor necrosis factor- α -inducible gene, SCC-S2, containing the consensus sequence of a death effector domain of fas-associated death domain-like interleukin-1 β -converting enzyme-inhibitory protein. *J Biol Chem* 2000; **275**: 2973–2978.
- Zhang LJ, Liu X, Gafken PR, Kioussi C, Leid M. A chicken ovalbumin upstream promoter transcription factor I (COUP-TFI) complex represses expression of the gene encoding tumor necrosis factor α -induced protein 8 (TNFAIP8). *J Biol Chem* 2009; **284**: 6156–6168.
- Liu T, Gao H, Chen X, Lou G, Gu L, Yang M et al. TNFAIP8 as a predictor of metastasis and a novel prognostic biomarker in patients with epithelial ovarian cancer. *Br J Cancer* 2013; **109**: 1685–1692.
- Zhang C, Kallakury BV, Ross JS, Mewani RR, Sheehan CE, Sakabe I et al. The significance of TNFAIP8 in prostate cancer response to radiation and docetaxel and disease recurrence. *Int J Cancer* 2013; **133**: 31–42.
- Hadisaputri YE, Miyazaki T, Suzuki S, Yokobori T, Kobayashi T, Tanaka N et al. TNFAIP8 overexpression: clinical relevance to esophageal squamous cell carcinoma. *Ann Surg Oncol* 2012; **19** (Suppl 3): S589–S596.
- Miao Z, Zhao T, Wang Z, Xu Y, Song Y, Wu J et al. SCC-S2 is overexpressed in colon cancers and regulates cell proliferation. *Tumour Biol* 2012; **33**: 2099–2106.
- Dong QZ, Zhao Y, Liu Y, Wang Y, Zhang PX, Jiang GY et al. Overexpression of SCC-S2 correlates with lymph node metastasis and poor prognosis in patients with non-small-cell lung cancer. *Cancer Sci* 2010; **101**: 1562–1569.
- Zhang C, Chakravarty D, Sakabe I, Mewani RR, Boudreau HE, Kumar D et al. Role of SCC-S2 in experimental metastasis and modulation of VEGFR-2, MMP-1, and MMP-9 expression. *Mol Ther* 2006; **13**: 947–955.
- You Z, Ouyang H, Lopatin D, Polver PJ, Wang CY. Nuclear factor- κ B-inducible death effector domain-containing protein suppresses tumor necrosis factor-mediated apoptosis by inhibiting caspase-8 activity. *J Biol Chem* 2001; **276**: 26398–26404.
- Shi TY, Cheng X, Yu KD, Sun MH, Shao ZM, Wang MY et al. Functional variants in TNFAIP8 associated with cervical cancer susceptibility and clinical outcomes. *Carcinogenesis* 2013; **34**: 770–778.
- Kruiswijk F, Labuschagne CF, Vousden KH. p53 in survival, death and metabolic health: a lifeguard with a licence to kill. *Nat Rev Mol Cell Biol* 2015; **16**: 393–405.
- Bieging KT, Mello SS, Attardi LD. Unravelling mechanisms of p53-mediated tumour suppression. *Nat Rev Cancer* 2014; **14**: 359–370.
- Li T, Kon N, Jiang L, Tan M, Ludwig T, Zhao Y et al. Tumor suppression in the absence of p53-mediated cell-cycle arrest, apoptosis, and senescence. *Cell* 2012; **149**: 1269–1283.
- Hager KM, Gu W. Understanding the non-canonical pathways involved in p53-mediated tumor suppression. *Carcinogenesis* 2014; **35**: 740–746.
- Valente LJ, Gray DH, Michalak EM, Pinon-Hofbauer J, Egle A, Scott CL et al. p53 efficiently suppresses tumor development in the complete absence of its cell-cycle inhibitory and proapoptotic effectors p21, Puma, and Noxa. *Cell Rep* 2013; **3**: 1339–1345.
- Menendez D, Inga A, Resnick MA. Potentiating the p53 network. *Discov Med* 2010; **10**: 94–100.
- Menendez D, Nguyen TA, Freudenberg JM, Mathew VJ, Anderson CW, Jothi R et al. Diverse stresses dramatically alter genome-wide p53 binding and transactivation landscape in human cancer cells. *Nucleic Acids Res* 2013; **41**: 7286–7301.

18. Allen MA, Andrysk Z, Dengler VL, Mellert HS, Guarnieri A, Freeman JA *et al*. Global analysis of p53-regulated transcription identifies its direct targets and unexpected regulatory mechanisms. *Elife* 2014; **3**: e02200.
19. Yang M, Zhao Q, Wang X, Liu T, Yao G, Lou C *et al*. TNFAIP8 overexpression is associated with lymph node metastasis and poor prognosis in intestinal-type gastric adenocarcinoma. *Histopathology* 2014; **65**: 517–526.
20. Liu T, Xia B, Lu Y, Xu Y, Lou G. TNFAIP8 overexpression is associated with platinum resistance in epithelial ovarian cancers with optimal cytoreduction. *Hum Pathol* 2014; **45**: 1251–1257.
21. Liu T, Gao H, Yang M, Zhao T, Liu Y, Lou G. Correlation of TNFAIP8 overexpression with the proliferation, metastasis, and disease-free survival in endometrial cancer. *Tumour Biol* 2014; **35**: 5805–5814.
22. Wang MC, Liu SX, Liu PB. Gene expression profile of multiple myeloma cell line treated by realgar. *J Exp Clin Cancer Res* 2006; **25**: 243–249.
23. Smeenk L, van Heeringen SJ, Koeppel M, van Driel MA, Bartels SJ, Akkers RC *et al*. Characterization of genome-wide p53-binding sites upon stress response. *Nucleic Acids Res* 2008; **36**: 3639–3654.
24. Menendez D, Inga A, Jordan JJ, Resnick MA. Changing the p53 master regulatory network: ELEMENTary, my dear Mr Watson. *Oncogene* 2007; **26**: 2191–2201.
25. Melo CA, Drost J, Wijchers PJ, van de Werken H, de Wit E, Oude Vrielink JA *et al*. eRNAs are required for p53-dependent enhancer activity and gene transcription. *Mol Cell* 2013; **49**: 524–535.
26. Harris SL, Levine AJ. The p53 pathway: positive and negative feedback loops. *Oncogene* 2005; **24**: 2899–2908.
27. Brooks CL, Gu W. The impact of acetylation and deacetylation on the p53 pathway. *Protein Cell* 2011; **2**: 456–462.
28. Salvador JM, Brown-Clay JD, Fornace AJ Jr. Gadd45 in stress signaling, cell cycle control, and apoptosis. *Adv Exp Med Biol* 2013; **793**: 1–19.
29. Romanov VS, Pospelov VA, Pospelova TV. Cyclin-dependent kinase inhibitor p21(Waf1): contemporary view on its role in senescence and oncogenesis. *Biochemistry (Mosc)* 2012; **77**: 575–584.
30. Moldovan GL, Pfander B, Jentsch S. PCNA the maestro of the replication fork. *Cell* 2007; **129**: 665–679.
31. Stacey DW. Cyclin D1 serves as a cell cycle regulatory switch in actively proliferating cells. *Curr Opin Cell Biol* 2003; **15**: 158–163.
32. Siu KT, Rosner MR, Minella AC. An integrated view of cyclin E function and regulation. *Cell Cycle* 2012; **11**: 57–64.
33. Yang K, Hitomi M, Stacey DW. Variations in cyclin D1 levels through the cell cycle determine the proliferative fate of a cell. *Cell Div* 2006; **1**: 32.
34. Del Sal G, Murphy M, Ruaro E, Lazarevic D, Levine AJ, Schneider C. Cyclin D1 and p21/waf1 are both involved in p53 growth suppression. *Oncogene* 1996; **12**: 177–185.
35. Chen X, Bargonetti J, Prives C. p53, through p21 (WAF1/CIP1), induces cyclin D1 synthesis. *Cancer Res* 1995; **55**: 4257–4263.
36. Manns J, Daubrawa M, Driessen S, Paasch F, Hoffmann N, Löffler A *et al*. Triggering of a novel intrinsic apoptosis pathway by the kinase inhibitor staurosporine: activation of caspase-9 in the absence of Apaf-1. *FASEB J* 2011; **25**: 3250–3261.
37. Ho CC, Siu WY, Lau A, Chan WM, Arooz T, Poon RY. Stalled replication induces p53 accumulation through distinct mechanisms from DNA damage checkpoint pathways. *Cancer Res* 2006; **66**: 2233–2241.
38. Muller PA, Vousden KH. Mutant p53 in cancer: new functions and therapeutic opportunities. *Cancer Cell* 2014; **25**: 304–317.
39. DiDonato JA, Mercurio F, Karin M. NF-kappaB and the link between inflammation and cancer. *Immunol Rev* 2012; **246**: 379–400.
40. Lowe J, Cha H, Lee MO, Mazur SJ, Appella E, Fornace AJ Jr. Regulation of the Wip1 phosphatase and its effects on the stress response. *Front Biosci (Landmark Ed)* 2012; **17**: 1480–1498.
41. Gudkov AV, Komarova EA. Dangerous habits of a security guard: the two faces of p53 as a drug target. *Hum Mol Genet* 2007; **16 (Spec No 1)**: R67–R72.
42. Zhang XY, Lu WY. Recent advances in lymphatic targeted drug delivery system for tumor metastasis. *Cancer Biol Med* 2014; **11**: 247–254.
43. Zimmerman ES, Heibeck TH, Gill A, Li X, Murray CJ, Madlansacay MR *et al*. Production of site-specific antibody-drug conjugates using optimized non-natural amino acids in a cell-free expression system. *Bioconjug Chem* 2014; **25**: 351–361.
44. Vassilev LT, Vu BT, Graves B, Carvajal D, Podlaski F, Filipovic Z *et al*. In vivo activation of the p53 pathway by small-molecule antagonists of MDM2. *Science* 2004; **303**: 844–848.
45. Liu X, Wilcken R, Joerger AC, Chuckowree IS, Amin J, Spencer J *et al*. Small molecule induced reactivation of mutant p53 in cancer cells. *Nucleic Acids Res* 2013; **41**: 6034–6044.
46. Selivanova G, Wiman KG. Reactivation of mutant p53: molecular mechanisms and therapeutic potential. *Oncogene* 2007; **26**: 2243–2254.
47. Hanahan D, Weinberg RA. Hallmarks of cancer: the next generation. *Cell* 2011; **144**: 646–674.
48. Lowe JM, Menendez D, Bushel PR, Shatz M, Kirk EL, Troester MA *et al*. p53 and NF-kappaB coregulate proinflammatory gene responses in human macrophages. *Cancer Res* 2014; **74**: 2182–2192.
49. Wassif CA, Krakowiak PA, Wright BS, Gewandter JS, Sterner AL, Javitt N *et al*. Residual cholesterol synthesis and simvastatin induction of cholesterol synthesis in Smith-Lemli-Opitz syndrome fibroblasts. *Mol Genet Metab* 2005; **85**: 96–107.
50. Menendez D, Shatz M, Azzam K, Garantziotis S, Fessler MB, Resnick MA. The Toll-like receptor gene family is integrated into human DNA damage and p53 networks. *PLoS Genet* 2011; **7**: e1001360.
51. Hagege H, Klous P, Braem C, Splinter E, Dekker J, Cathala G *et al*. Quantitative analysis of chromosome conformation capture assays (3C-qPCR). *Nat Protoc* 2007; **2**: 1722–1733.

Supplementary Information accompanies this paper on Cell Death and Differentiation website (<http://www.nature.com/cdd>)